

Summary

Motivation Neurons depend critically on active transport of cargoes throughout their complex neurite networks for their survival and function. Defects in this process have been strongly associated with many human neurodevelopmental and neurodegenerative diseases. To understand related neuronal physiology and disease mechanisms, it is essential to measure the traffic flow within the neurite networks. Currently, however, image analysis methods required for this measurement are lacking.

Results We developed a method that is capable of measuring the flow rates of cargo traffic at any specified locations along individual branches of the neurite networks. A main focus of our method development is robust performance, which ensures that our method works reliably and accurately under low signal-to-noise ratios. We validated and benchmarked our method using both synthetic and actual image data and found its accuracy to be >85% on average under normal conditions.

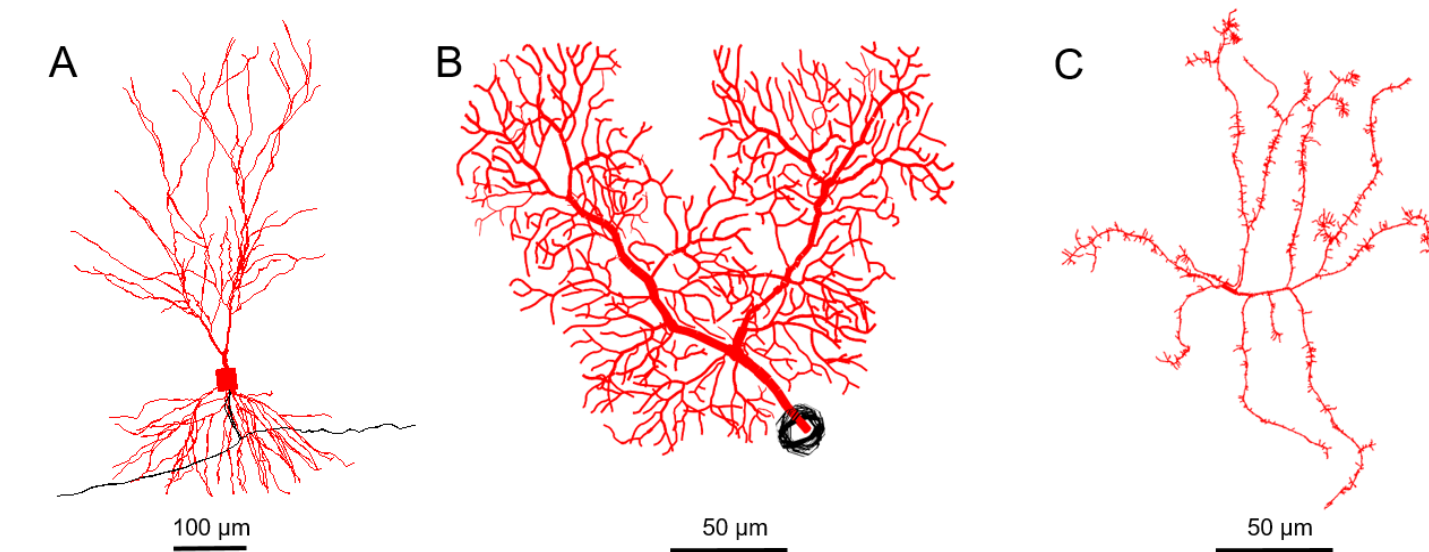


Figure 1. Selected examples of complex geometry of neurite networks. All examples are from the NeuroMorpho database [1]. Soma and axons: black; dendrites: red. (A) Rat pyramidal neuron (NMO_00218). (B) Mouse cerebellum Purkinje neuron (NMO_35058). (C) Drosophila multidendritic-dendritic arborization class III neuron (NMO_06962).

Methods

2D time-lapse image sequences

Extraction of network geometry by neurite tracing

Specification of locations for measurement of traffic flow

Generation of kymograph

Computational removal of background & stationary cargo trajectories from kymograph

Detecting & counting cargo trajectories through specified locations

Output of measurements of traffic flow

Experimental data collection

In this study, we used primarily time-lapse movies of transport of APP (amyloid precursor protein) vesicles in cultured rat hippocampal neurons for developing, validating and benchmarking our method. Time-lapse movies of YFP labeled APP vesicles were collected at 10 frame per second.

Computational removal of background and stationary cargo trajectories

The removal process serves two purposes. First, it reduces the background fluorescence level and increases the SNR (Fig. 3C). For example, the kymograph in Fig. 3B has an SNR of 4.7. After background removal by the method in [2], the SNR is increased to 7.0 (Fig. 3C). Second, it removes trajectories of stationary cargoes (Fig. 3D) and, therefore, simplifies subsequent detection and analysis of trajectories of moving cargoes.

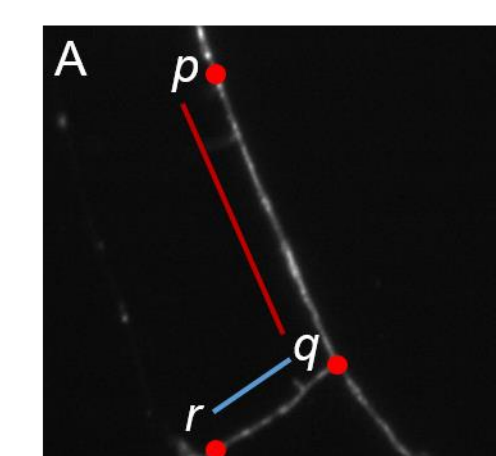


Figure 3. Kymograph background removal. (A) A representative neurite junction, a basic element of the neurite network structure. (B) Raw kymograph over pq and qr before background removal; (C) Kymograph after background removal. (D) Removed background, including stationary cargo trajectories.

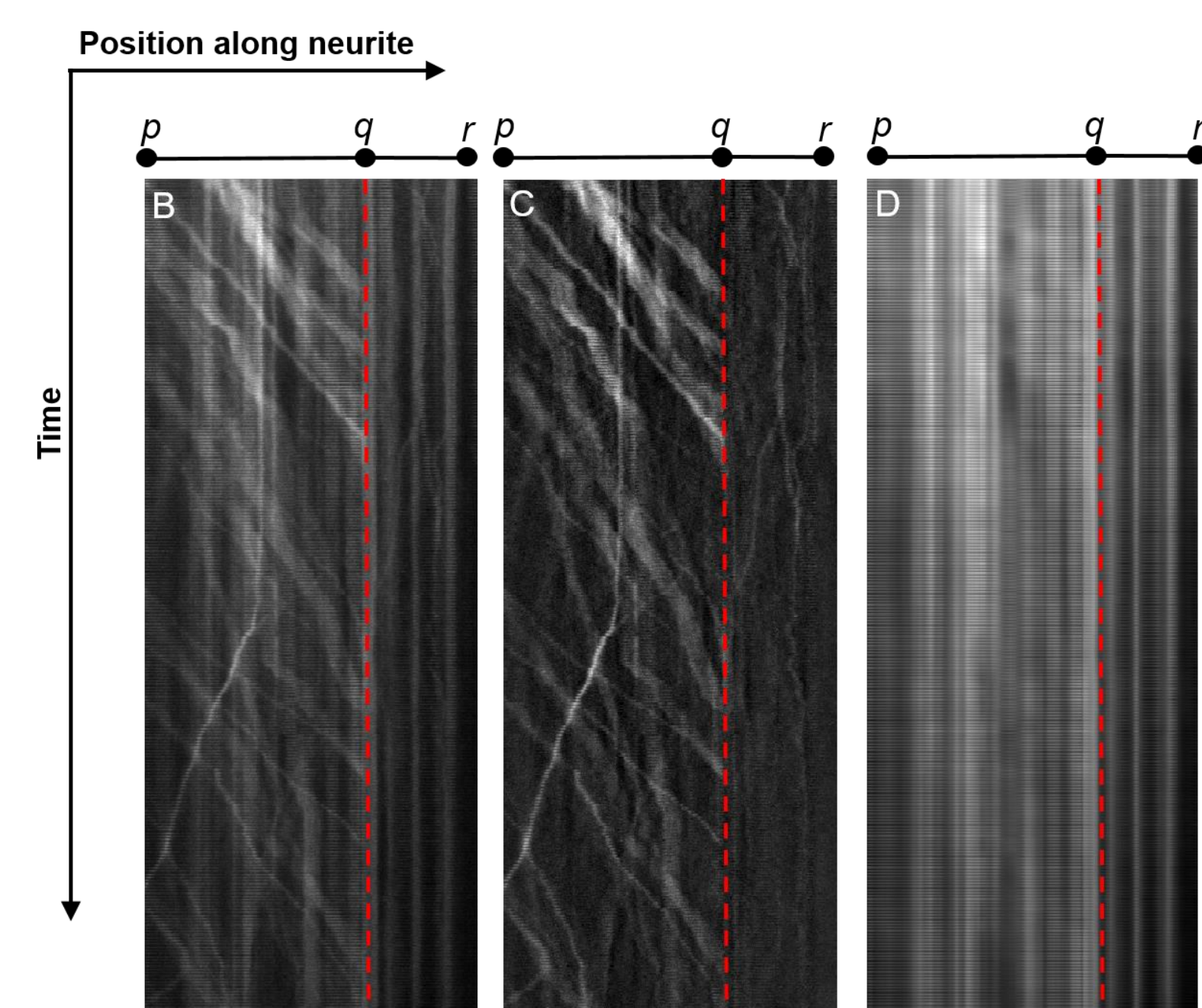


Figure 2. Overview of workflow

Methods

Detecting and counting cargo trajectories

Following background removal, we detected cargo trajectories in the kymograph using Steger's curve detection algorithm [3]. Then a specified location of observation is established. The numbers of cargoes passing through it can be determined by counting the trajectory segments passing the vertical line. We developed a sliding-window strategy that can effectively suppress the fluctuation in flow rate estimation caused by broken detection results, enhancing the robustness of the method.

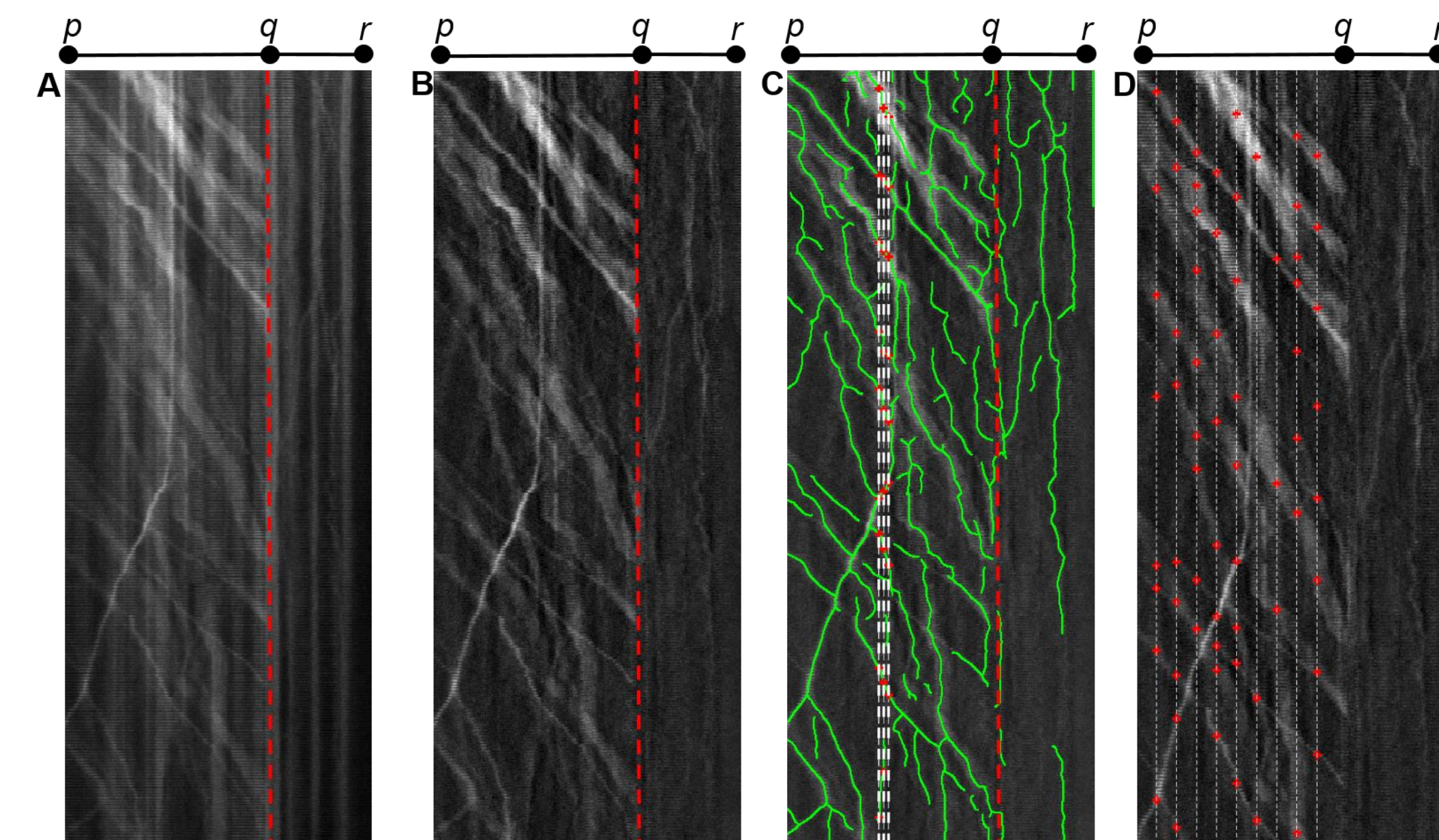


Figure 4. Cargo trajectory detection. (A) Raw kymograph, same as Fig. 3B (B) After background removal (C) Detected trajectories shown in green overlaid. (D) Measurement results at 9 locations with a spacing of 20 pixels (1.29 μm).

Result I. Experiments using synthetic images

To test our method, we generated synthetic images of cargo transport in a single neurite under different signal-to-noise ratios and spatial densities. We define the accuracy as the following.

$$\text{Accuracy} = \left(1 - \frac{|N_{\text{Measured}} - N_{\text{Groundtruth}}|}{N_{\text{Groundtruth}}}\right) \times 100\%$$

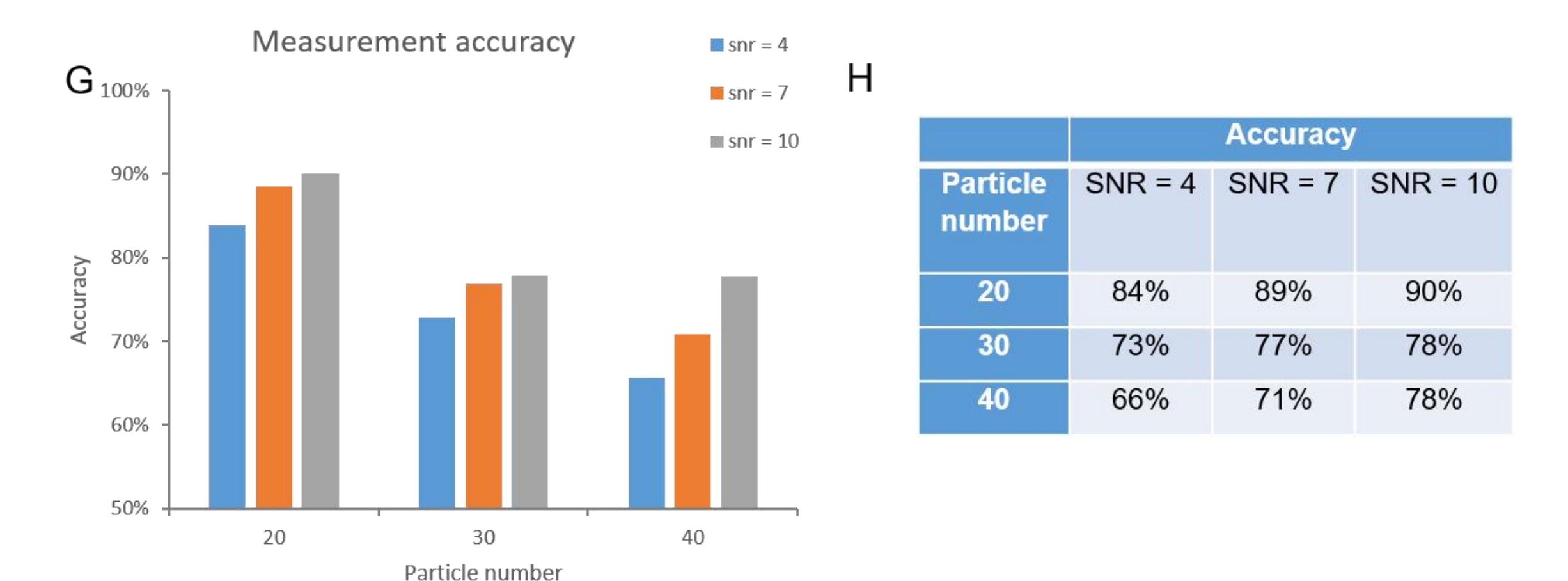
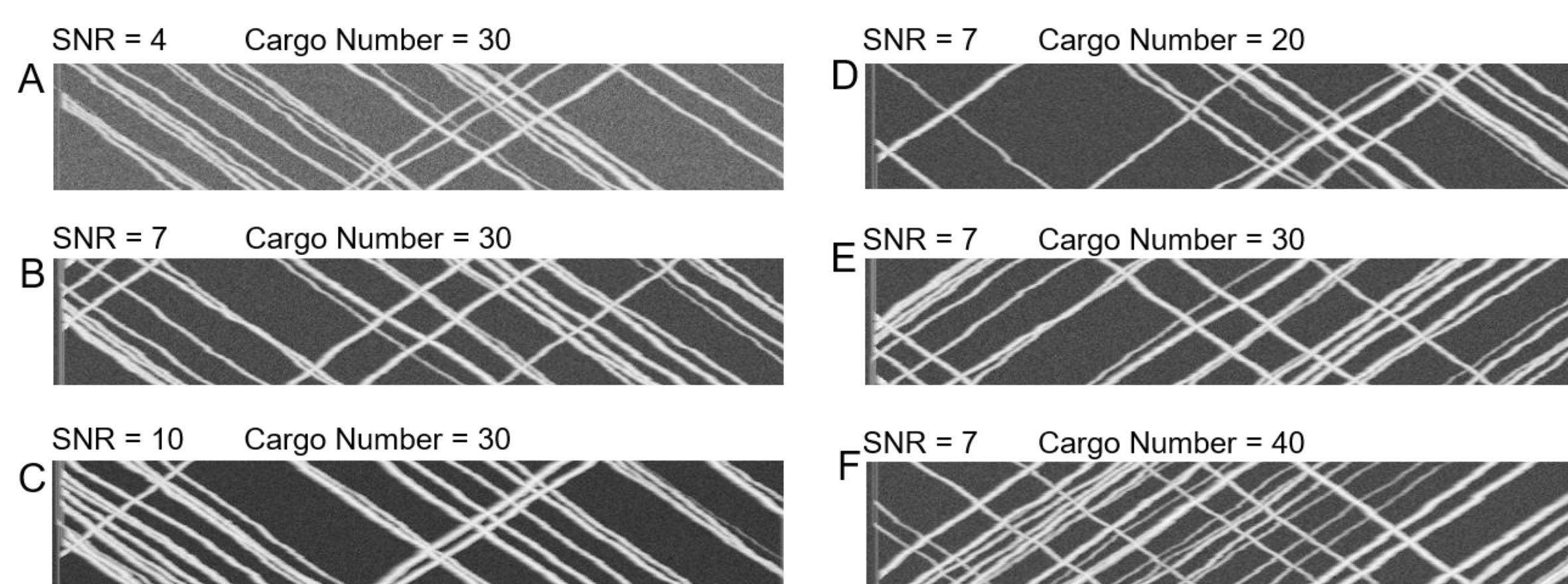


Figure 5. Summary of experimental results using synthetic data. (A-C) Representative kymographs generated from synthetic images. Cargo number is kept at 30. Signal to noise varies from 4 to 7. (D-F) Signal to noise is kept at 7, cargo number changes from 20 to 40. (G) Bar plot comparing measurement accuracies under different conditions. (H) A table comparing measurement accuracies under different conditions.

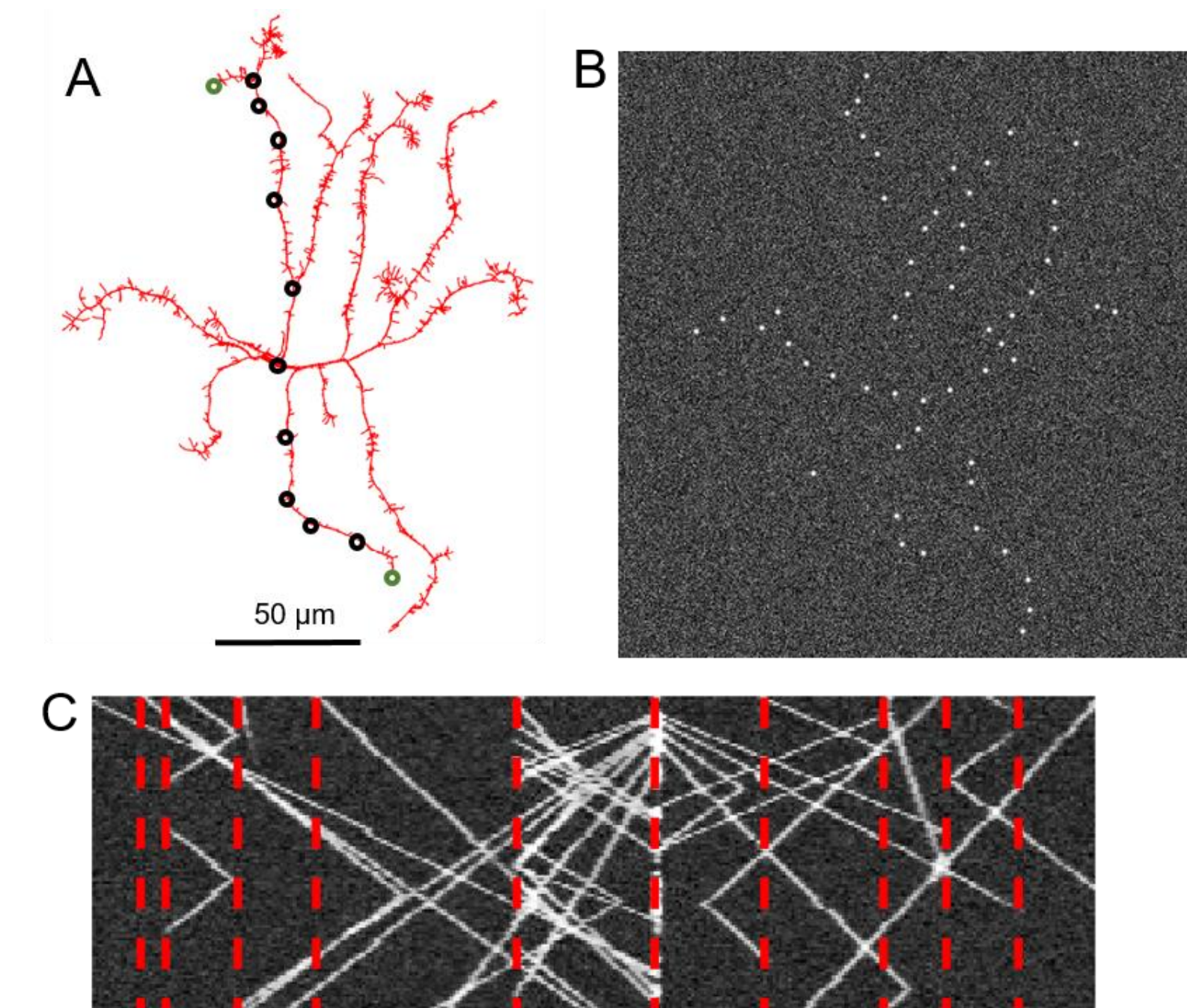
Result II. Experiments using real images

Table 1. Summary of analysis results for the example show in Figure 4.

Observation Location	Ground truth	Algorithm count	Accuracy
20	10	8	80%
40	10	9	90%
60	9	10	89%
80	9	8	89%
100	9	8	89%
120	8	4	50%
140	8	5	63%
160	9	9	100%
180	9	10	89%

To further test the method, we have also used it to analyze the real image in Figure 4. The ground truth was from manually counting.

Result III. Synthetic images of complex neurite networks



We have thus far tested our method under relatively simple neurite geometry. Our method can be used to measure traffic flow not just within individual neurite branches but also over different branches.

Figure 6. Synthetic images of cargo transport in a neurite network (A) Network geometry used for generating synthetic images of cargo traffic, same as Fig. 1C. (B) A representative frame of generated synthetic images. (C) Kymograph was generated from top to bottom along the connected neurites between the two green circles. Red dotted lines correspond to junction points marked by the black circles in (A).

Conclusions

- In this study we developed a method that measures traffic flow rates at any specified locations in complex neurite networks. To ensure robust performance under low SNRs, we used two strategies. First, we applied our computational background removal algorithm to improve SNRs. Second, we used a sliding-window in counting trajectories to resolve at least partially the issue of fragmentation in trajectory detection. We tested our method using both synthetic and real image data and found that on average it can achieve >85% accuracy.
- Our method also has its limitations. First, its accuracy may drop substantially when multiple trajectories converge. Our goal is to optimize our method specifically to resolve such cases. Second, our method depends critically on the performance of the Steger's curve detection algorithm, whose performance degrades when the spatial density of trajectories is high due to its design to use a large isotropic Gaussian kernel for image filtering.

References

- G. A. Ascoli, D. E. Donohue, and M. Halavi, "NeuroMorpho.Org: a central resource for neuronal morphologies," *Journal of Neuroscience*, vol. 27, pp. 9247-9251, 2007.
- H.-C. Lee and G. Yang, "Computational removal of background fluorescence for biological fluorescence microscopy," in *2014 IEEE 11th International Symposium on Biomedical Imaging (ISBI) 2014*, pp. 205-208.
- C. Steger, "An Unbiased Detector of Curvilinear Structures," *IEEE Trans. Pattern Anal. Mach. Intell.*, vol. 20, pp. 113-125, 1998.

Acknowledgements

X.C. acknowledges a Ji-Dian Liang Graduate Research Fellowship. Y.J.Z. acknowledges NSF Faculty Career grant OCI-1149591. G.Y. acknowledges NSF Faculty Career grant DBI-1149494. Y.J.Z. and G.Y. also acknowledge a CMU Department of Mechanical Engineering seed grant for this project